ELSEVIER

Ceramics International 30 (2004) 311–332

CERAMICS INTERNATIONAL

www.elsevier.com/locate/ceramint

Review

Some aspects in self-propagating high-temperature synthesis

P. Mossino*

Materials Science and Chemical Engineering Department, Politecnico of Turin, Turin 10129, Italy

Received 4 April 2003; received in revised form 20 May 2003; accepted 3 June 2003

Abstract

A general and historical review of the SHS process (Self-propagating High-temperature Synthesis) has been considered. The influence of reaction parameters such as particle size, stoichiometry of the reactants, pellet size and green density, gas pressure, is reported. Improvements of SHS processes for reactions that are not so exothermic to propagate are examined. The final part of the work underlines the economical and environmental impact of SHS process.

Keywords: SHS; Reaction parameters; Economical and environmental impact

Contents

* Tel.: +39-011-564-4702; fax: +39-011-564-4699.
E-mail address: peircarla.mossino@polito.it (P. Mossino).

0272-8842/$30.00
doi:10.1016/S0272-8842(03)00119-6

1. Introduction

Development of efficient and energy-saving technologies is of great importance today. Self-propagating High-temperature Synthesis (SHS) is a relatively novel and simple method for making certain advanced ceramic, composites and intermetallic compounds. This method has received considerable attention as an alternative to conventional furnace technology [1].

The SHS is based on systems able to react exothermally when ignited and to sustain them to form a combustion wave. The temperature of the combustion can be very high (as 5000 K) and the rate of wave propagation can be very rapid (as 25 cm/s), hence this process offers the opportunity to investigate reactions in conditions of extreme thermal gradients (as 10^5 K/cm).

Fig. 1 shows schematically the combustion wave, which progressed trough the sample leaving behind the products of combustion [2].

In the typical combustion synthesis the reactants are usually fine powders, mixed and pressed into a pellet to increase an intimate contact between these. The reactant mixture is placed in a refractory container and ignited in vacuum or inert atmosphere [1]. The products of the reaction are extremely porous, typically 50% of theoretical density [3].

Reactions between particulate materials are an alternative way to produce various types of materials

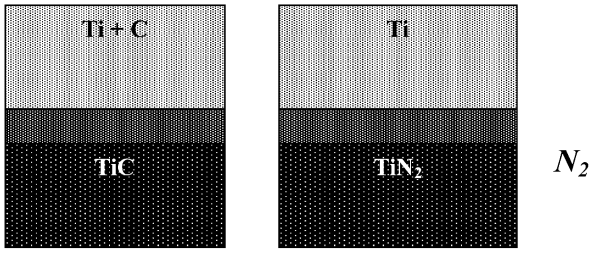

Fig. 1. Schematic representation of SHS reaction: (a) solid–solid (Ti + C) and b) solid–gas (Ti + N_2).

considering the extreme simplicity of the process, relatively low energy requirement, high purity of the products obtained, the possibility to obtain metastable phases, and the possibility of simultaneous synthesis and densification. Higher purity of products is the consequence of high temperature associated to the combustion, volatile impurities are expelled as the wave propagates through the sample. The possibility of the formation of metastable phases is based on high thermal gradients and rapid cooling rate associated with the reaction [2].

2. Materials and applications

Two approaches are being used in SHS technology; the first of them is the production of intermediate products, which are then used as raw materials in further processing; the second approach is based on direct production of finished article, in this case synthesis, structuring and shaping are carried out in a one-stage (simultaneous synthesis and densification) [4].

Actually over 500 compounds have been synthesising by SHS method. Some of these materials are listed in Table 1.

The applications of these materials can be classified as:

- Abrasives, cutting tools and polishing powders.
- Resistive heating elements.
- Shape-memory alloys.
- High temperature intermetallic compounds.
- Steel processing additives (nitrided ferroalloys).
- Electrodes for electrolysis of corrosive media.
- Coatings for containment of liquid metals and corrosive media (products of iron oxide and aluminium thermite reaction).
- Powder for further ceramic processing.
- Thin film and coatings.

Table 1
Some materials produced by SHS [3]

Borides	CrB, HfB, NbB, NbB_2, TaB_2, TiB, LaB_6, MoB, MoB_2, MoB_4, Mo_2B, WB, W_2B_5, WB_4, ZrB_2, VB, V_3B_2, VB_2
Carbides	TiC, ZrC, HfC, NbC, SiC, Cr_3C_2, B_4C, WC, TaC, Ta_2C, VC, Al_4C, Mo_2C
Nitrides	Mg_3N_2, BN, AlN, SiN, Si_3N_4, TiN, ZrN, HfN, VN, NbN, Ta_2N, TaN
Aluminides	NiAl, CoAl, $NbAl_3$
Silicides	TiS_3, Ti_5Si_3, ZrSi, Zr_5Si_3, $MoSi_2$, $TaSi_2$, Nb_5Si_3, $NbSi_2$, WSi_2, V_5Si_3
Hydrides	TiH_2, ZrH_2, NbH_2,CsH_2, PrH_2, IH_2
Intermetallics	NiAl, FeAl, NbGe, $NbGe_2$, TiNi, CoTi, CuAl
Carbonitrides	TiC–TiN, NbC–NbN, TaC–TaN, ZrC–ZrN
Cemented carbides	TiC–Ni, TiC–(Ni, Mo), WC–Co, Cr_3C–(Ni,Mo)
Chalcogenides	MgS, $NbSe_2$,$TaSe_2$, MoS_2, $MoSe_2$, WS_2, WSe_2
Binary compounds	TiB_2–MoB_2, TiB_2–CrB_2, ZrB_2–CrB_2, TiC–WC, TiN–ZrN, MoS_2–NbS_2, WS_2–NbS_2
Composites	TiB_2–Al_2O_3, TiC–Al_2O_3, B_4C–Al_2O_3, TiN–Al_2O_3, TiC–TiB_2, $MoSi_2$–Al_2O_3, MoB–Al_2O_3, Cr_2C_3–Al_2O_3, 6VN–5Al_2O_3, ZrO_2–Al_2O_3–2Nb

- Functionally graded materials.
- Composite materials.
- Materials with specific properties [3].

The SHS process has a good control of the chemical composition, so a new application of materials product by SHS process can be Thermal Spray [5].

Another recent application of SHS technique is the synthesis of lithium nickelate ($Li_{0.88}Ni_{1.12}O_2$), lithium cobaltate ($LiCoO_2$) and lithium manganate ($LiMn_2O_4$); these compounds are three most popular 4 V cathode materials tested in lithium-ion batteries. For this synthesis the stoichiometries of the reaction mixture were taken as follows:

$$LiNO_3 + Co(NO_3)_2 + 2.5\ NH_2–CO–NH_2$$
$$LiNO_3 + Ni(NO_3)_2 + 2.5\ NH_2–CO–NH_2$$
$$LiNO_3 + 2Mn(NO_3)_2 + 4.2\ NH_2–CO–NH_2$$

The nitrate is responsible for the oxidation of urea to yield a high temperature, and also for the oxidation of the transition metals [6].

Recently the production of composite thin films is becoming more important in the engineering of surfaces; the combustion synthesis provides an alternative way for the production of composite targets used in the sputtering of composite films. For example it can consider the production of TiC–TiB_2 composite targets, which could be used in sputtering thin films. This target is produce with the application of uniaxial pressure during the reaction, and after it is possible sputter it in order to produce a film. The film produced has high thermal stability [7].

3. Fundamental reaction parameters

There are a number of reaction parameters in SHS process such: particle size, stoichiometry of the reactants, green density, gas pressure, size of the pellets, ignition mode; all are fundamental in SHS process. All of these parameters have an effect on the combustion products, and varying one of this is possible that a reaction propagates or not.

3.1. Effect of particle size

Particle size of the reactant powder has a strong effect on SHS process. The particle size of the reactants influences the degree of completation of the reaction, the temporal sequence of the reaction, the temperature profile of the combustion zone and the velocity of the combustion wave [2].

Concerning the relationship between wave velocity and particle size, an explicit expression for the rate of the SHS reaction needs to be incorporated into Fourier heat balance relationship:

$$k\frac{\partial^2 T}{\partial x^2} - C_p\rho\frac{\partial T}{\partial x} + Q\frac{\partial \eta}{\partial t} = 0 \tag{1}$$

where k, C_p, and ρ are respectively: the thermal conductivity, the heat capacity and the density; Q is the heat of the reaction, η is the degree of advancement of the reaction, T is temperature, t is time and x is the axis of wave propagation. Some authors provided the first analysis for the relationship between wave velocity and reaction rate, in doing so they examined two cases: (a) the reaction is homogeneous and takes place in a narrow region and (b) the reaction in not completed in the front but continues well beyond the passage of the wave. For first case an expression for the wave propagation velocity v vas derived as:

$$v^2 = f(n)\frac{kC_p}{\rho Q}\frac{RT_N^2}{E}k_0\exp\left(-\frac{E}{RT}\right) \tag{2}$$

where $f(n)$ is a kinetic function of the order of the reaction, n; k_0 is a constant, E is the activation energy for the reaction, R is the gas constant, T_N is the combustion temperature, and the other symbols are defined in Eq (1).

Implied in the assumption regarding the nature of the reaction is that the velocity is independent of particle size and of other similar materials characteristics. However, in case (b), the fact that the reaction is not complete within the combustion zone suggests the presence as the diffusion of reactants through a product layer.

For this case, the effect of particle size is included in different models of heterogeneous reactions where the reaction rate is controlled by diffusion. In order to determine the reaction rate, $\partial\eta/\partial t$ it is necessary to assume a certain geometry for the distribution of reactants and products.

Some authors used geometry of alternating layers of reactants, parallel to wave propagation direction and assumed reaction kinetics controlled by diffusion of the reactants through the layer of reaction products. Their analyses resulted in the following velocity expression:

$$v^2 = \frac{2k}{a_0^2 w C_p\rho}D_0\exp\left(-\frac{E}{RT}\right) \tag{3}$$

where a_0 is the initial layer thickness of one of the reactants, that is related the thickness of the other by the reaction stoichiometric ratio $w = 1 + b_0/a_0$ being the thickness of the layer of the second reactant. Also D_0 is the diffusion coefficient preexponential, and E is the diffusion activation energy.

Using the same geometry as above, but with a different model of diffusion and different function for the

temperature profile, was obtained the following expression for the effect of layer thickness on propagation velocity:

$$v^2 = \frac{6RT_c^2}{l^2E(T_c - T_0)} D_{\text{eff}} k_{\text{eff}} \cong \frac{6RT_c}{l^2E} k_{\text{eff}} D_0 \exp\left(-\frac{E_{\text{eff}}}{RT_c}\right) \quad (4)$$

where l is the thickness of two adjacent reactant layers, D_{eff} is the effective diffusion coefficient, k_{eff} is the effective thermal conductivity, T_c is the combustion temperature, and T_0 is the ambient temperature.

Other authors also considered the effect of the particle size distribution on the degree of conversion. Assuming a parabolic law controlling the reaction rate and a narrow reaction zone, they derived a relationship for the wave velocity as:

$$v^2 = \frac{6k}{l_{\text{eff}}^2} \frac{RT_c^2}{EQ} k_0 \exp\left(-\frac{E}{RT_c}\right) \quad (5)$$

where

$$l_{\text{eff}}^2 = \int_{l_1}^{l_2} l^2 \chi(l) dl \quad (6)$$

which represents the effective heterogeneity size or particle size with $\chi(l)$ being the particle size distribution function; l_1 and l_2 are the smallest and largest particle size, respectively.

Another aspect of the effect of particle size of reactants is that related to systems in which typically a metallic reactant melts in the propagation front. The kinetics of subsequent reaction is enhanced but the melting is controlled by the reaction of the liquid with the solid phase.

Another author analysed a model where one reactant melts and surrounds the solid spherical particles of the other reactant. Two mechanisms for reaction kinetics control were considered: the diffusion of the liquid reactant through a surface layer of solid reactions product and kinetics of reaction at the surface of the solid reactant. For both cases, the reaction rate is dependent on the particle size of the solid reactant.

Assuming a planar steady-state wave with the reaction being completed in a narrow zone, the dependence of velocity on particle size was derived as:

$$v^2 = \frac{k}{Q\rho} \frac{RT_c^2}{E} \frac{k_0 \exp\left(-\frac{E}{RT}\right)}{f(\eta)} A \quad (7)$$

with

$$A = \frac{3C}{a\rho r} \quad (8)$$

for surface-reaction-controlled kinetics, and

$$A = \frac{3C}{a\rho r^2} \quad (9)$$

for diffusion-controlled kinetics, where $f(\eta)$ is a kinetics function, C is the initial mass fraction solid reactants in the mixture, ρ is the reactant compact density, r is the solid particles radius, and a is the stoichiometric ratio. For total conversion inside the reaction zone $\eta = 1$ and $f(\eta) = 1/4$ for diffusion-controlled kinetics and $f(\eta) = 3/4$ for surface-reaction-controlled kinetics. Again, the effect of particle size appears in the pre-exponential term of the propagation velocity equation.

The relationship $1/r$ was confirmed for diffusion-controlled reaction kinetics but the relationship $1/r^{1/2}$, proposed when the kinetics are controlled by the reaction at the surface, is yet to be demonstrated [8].

Also in the case of the reaction between two elements that one is a low melting element (the metal), same authors supposed that the predominant mode depends on the particle size of metal, so they consider two modes of combustion: diffusion mode and capillary mode.

In the diffusion mode diffusional processes between the reactants control the reaction, while in the capillary mode the combustion reaction is controlled by the rate of capillary spreading of the molten phase through the particle of non-melting reactant. Experimental measurement has shown that the diffusional mode is predominant when the particle size is small and the condition over this mode exists can be expressed as:

$$r_0^2 \ll \sigma\lambda r_r \mu V^2 \ln\left[\frac{(T_c - T_0)}{(T_m - T_0)}\right] \quad (10)$$

where r_0 is the particle size of the starting metal component, r_r is the particle size of the refractory non molten component, λ is the thermal diffusivity, σ is the surface tension of the liquid, μ is the viscosity of the liquid, V is the velocity of the combustion front, T_c is the combustion temperature, T_m is the melting point of the molten component and T_0 is the pre-heating temperature or the initial temperature. The condition over which the capillary mode is dominant is:

$$r_0 \gg \frac{\sigma r_r}{\mu D} \quad (11)$$

where D is the diffusion coefficient of the reactant in the product.

The relationship between the particle size and the velocity is show in Fig. 2.

These curves are obtained for the reaction between titanium and carbon; in particular, the curves are derived for three particle sizes of carbon. There are three regions represented in this diagram: I, kinetic

region where the diffusion controlled mode is dominant and the velocity is independent of r_0 (size particle of metallic component); II, the transition region where V dramatically decreases as r_0 increases; III the capillary region, where the dependence of V on r_0 is relatively weak. In this case the combustion temperature and the propagation velocity of the combustion wave decrease as the particle size of Ti (melting component) increases [3].

Considering the case of SiC a very fine size of the carbon reactant (non-melting component) is not required and not advantageous. Fine particles loose heat more readily than the larger ones and this is equivalent to decrease of thermal conductivity and to inhibit the propagation of the combustion zone; the effect of to small particle size can be offset by an increase of thermal conductivity. For the silicon a small size is required [9,10].

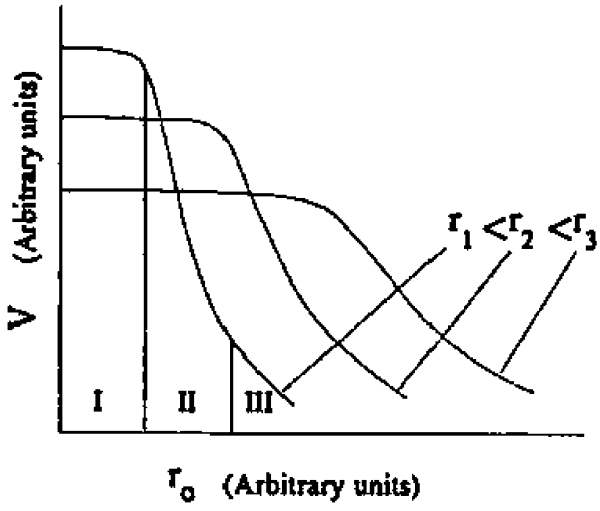

Fig. 2. Dependence of the combustion rate to the particle size of metallic (r_0) and non-metallic (r_1, r_2, r_3) reactants (I) kinetic region; (II) transition region; (III) capillary region [3].

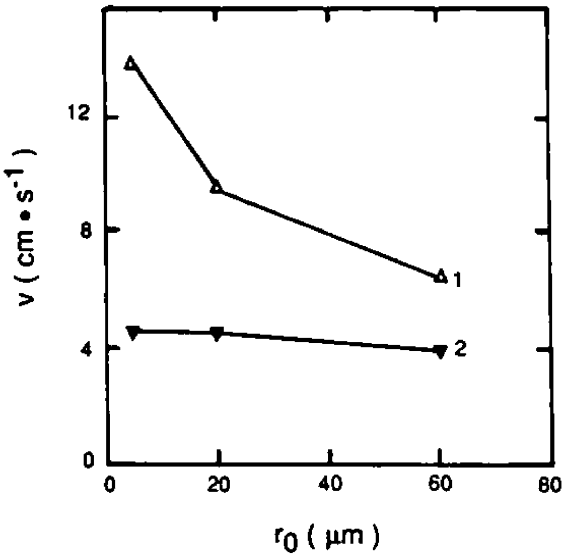

Fig. 3. The effect of aluminium particle size on the combustion rate of Ni–Al mixture (1) fine-grained and (2) coarse-grained Ni particles $\rho_r = 40\%$ [2].

In the synthesis of nickel monoaluminide (NiAl) it was concluded that particles size of both reactants are important in determining the velocity of the combustion because the two are molten in the reaction zone. Fig. 3 shows that the velocity of the wave decreases with increasing aluminium particle size if fine nickel particles are used, but is essentially independent of r_{Al} if coarse particles of Ni are used. A similar trend of decreasing velocity with increasing particle size was observed in the synthesis of TiNi [2].

Considering the dependence of the combustion temperature and the wave propagation velocity of the Ti particle in the synthesis of TiC, the maximum temperature and the velocity of the combustion decrease as the titanium particle size increase. Along with a decrease in the maximum combustion temperature a more interesting evidence of changes in the combustion process resulting from an increase in particle size is demonstrated in Fig. 4.

Not only does the maximum temperature decrease but also the temperature profile of the combustion front broadens as r_0 increases, indicating that the combustion reaction is taking place over a wider region of the sample. Thus the broadening of the reaction front is a consequence of a decrease in the degree of completeness of the reaction as a result of an increase in particle size of Ti and not a decrease in the combustion temperature [2].

Considering the gas–solid reactions its has been demonstrated experimentally that the particle size and shape became significant parameters; combustion temperature and rate of the combustion wave decreased with decreasing pore size in the green compact [3].

The particle size also influences the nature of the products, in particular the size of starting powder had an effect on the grain size of the resulting products that

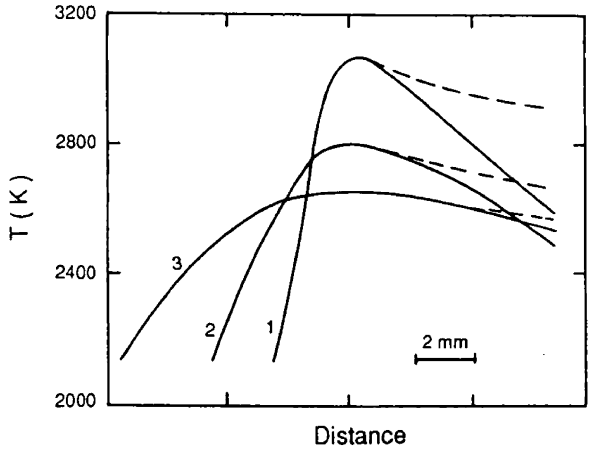

Fig. 4. Temperature profile along the sample during the combustion for Ti + C mixture with different particle of titanium: (1) r_0 <45 μm, (2) r_0 = 120-160 μm, (3) r_0 = 250–280 μm [2].

decreased with a decrease in the particle size of starting powders [2].

3.2. Compaction of green powders

The compactation of the green powders plays an important role in the combustion synthesis reaction.

The compact ability of the system depends directly on the properties of the materials such as hardness and strength. If the particles are not very hard they have a higher degree of compaction. Generally the large particles produce a higher packing density and exhibit higher density at all compaction pressures, the small particles are more difficult to compact. A wide particle size distribution will increase the density at any compaction pressure.

A green compact produced with significantly high or low densities which ignite with difficulty. This effect of green density on the ignition and propagation of the reaction was attributed to the balance between a good particle contact but not too much to lead to excessive heat loss from the reaction zone due to increased thermal conductivity [3].

The porosity of the sample also has an effect on the capillary spreading; in particular a maximum benefit from spreading is attained when the molten phase fills completely the voids in the sample. Thus the optimum density of the sample is one in which the volume fraction of the pores is approximately equal to the volume fraction of the molten metal. Lower metal volume fractions lead to the partial filling of the pores and hence a lower degree of contact between the reactants, but a higher metal volume fraction leads to the formation of excess liquid, beyond what is necessary to fill the pores. In both cases the intensity of the reaction is diminished leading expectedly to a decrease in the combustion temperature. It is possible calculate the ideal relative density on the basis of equating the volume of the molten metal and voids in the sample. The following relationship provides this calculation for one mole of refractory compound with formula MX_a where M is the metal and X the non-metal and a the stoichiometry coefficient:

$$\rho_c = \frac{b(m_M\rho_X + am_X\rho_X)}{(1+b)m_H\rho_X + abm_X\rho_M} \tag{12}$$

where ρ_c is the ideal starting mixture relative density of the metal and non-metal, m_H and m_X are the atomic masses of the metal and non-metal and ρ_M and ρ_X are the densities of the metal and non-metal, respectively and b is the density ratio of the metal in the liquid state to that in the solid state [2].

For example in the synthesis of W from WO_3 and Zn the effect of green density of the compact is show in Fig. 5, as the green density increased from the bulk value 2950 to 4600 kg/m^3, the combustion velocity decreased and the sample swelling increased. When $\rho > 4600$ kg/m^3 the combustion flame extinguished immediately after ignition. The reason for the combustion temperature decrease at dense green pellet has been accepted as the heat loss at combustion front because the effective thermal conductivity increases as the porosity decreases. In this experiment, however, both the combustion temperature and velocity may be decreased due to the decrease of the permeability. The diameter of the samples did not change after the combustion. On the lateral surface of the samples with higher density, the traces of the spin combustion and cracks were observed. This may be because the permeability of the compacts decreased as the density increased and then the pressurised Zn vapour boiled out from inside the sample to the surface, leaving cracks [11].

In the case of the gas–solid reaction, for example considering the synthesis of AlN, the degree of conversion of the reactant decrease with an increase of the green density, this is due to the decrease of the local availability of N_2 if the pore volume decreases [1].

Also in the synthesis of $Ni_{0.35}Zn_{0.65}Fe_2O_4$ nickel-zinc ferrites (starting from powder of iron, iron oxide, nickel oxide, and zinc oxide) with the increase of relative density of raw materials, a decrease of T_c and V_c (velocity of combustion wave) is observed. This is because the oxygen has difficulty in penetrating into the crystal structure of reactants. When the relative density is above 60% the combustion reaction will extinguish due to low oxygen presence in the reaction zone. In Fig. 6 is represented the variation of T_c and U_c vs. density [12].

In some cases, synthesis of TiN, the velocity of the wave decreases if the porosity decreases as a consequence of the melting of titanium that removes heat from the combustion front and ultimately causes a non-steady-state combustion mode [2,13]. The porosity of the products depends of the initial relative density of the titanium compacts. In general porosity of the products depends on three factors: the initial relative density, the

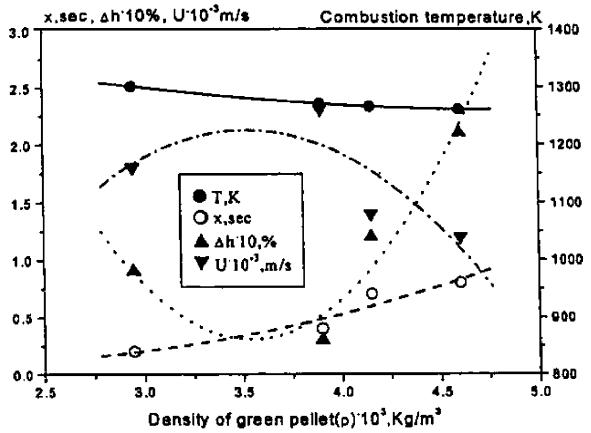

Fig. 5. Effect of green pellet density on the combustion parameters, where U is the combustion velocity Δh is the swelling [11].

difference in the molar density of the reactant and products and the evolution of impurity gases during combustion, in this case the final porosity is influenced by the degree of melting of titanium [13].

Also in the case of the synthesis of Si_3N_4, comparison of the samples with 60 and 80% porosity data reveal a higher combustion velocity for 80% porosity samples with 60% porosity. This effect may be due to two reasons. The coalescence of the melted Si particles is favoured by an increase in the packing density. This phenomenon leads to lower combustion velocity. The second reason is that an increase in the packing density of the green mixture causes an increase of thermal diffusivity [14].

Another important element is the size of the pellet. It was observed for the synthesis reaction of TiB_2 that no reaction could be initiated and sustained when the specimen had a small diameter, because the radial heat losses increase [15,16].

In particular considering the variation of the thickness of the sample between 0.1 and 10 mm for 80 mm long, when the thickness increases from 0.15 to 2 mm the temperature rises from 2000 to 2800 °C, when $\delta > 2$ mm the maximum combustion temperature remains unchanged for quite a long time.

Fig. 7 presents the dependence of the maximum combustion temperature on the thickness. The dependence of the combustion rate on the sample thickness is shown in Fig. 8. In this curve there is a presence of a maximum of combustion rate that is observed when $\delta = 2$ mm as results from the combined actions of heat losses and degassing. When the sample thickness is decreased $\delta < 2$ mm, the combustion rate falls of because the intensity of external heat losses grows. The critical combustion rate is 12 cm/s. under the action of various factors; the front of glasses combustion undergoes changes.

In Fig. 9 is shown the variation of the temperature profile. The temperature behind the reaction front drops abruptly, during the combustion of a thin sample caused by a high level of heat losses. Under these conditions, the after-combustion zone is practically absent. When the pellet thickness increases from 0.2 to 1.8 mm

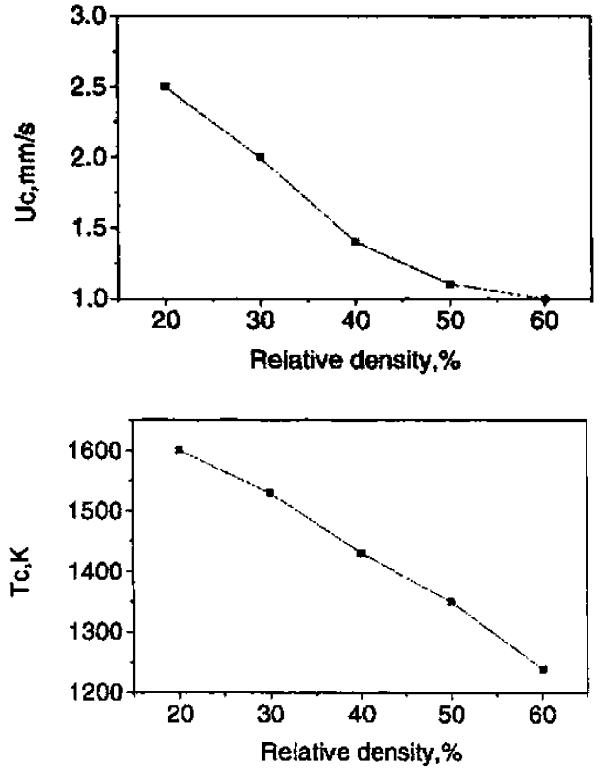

Fig. 6. T_c and U_c (velocity) vs relative density of raw materials [12].

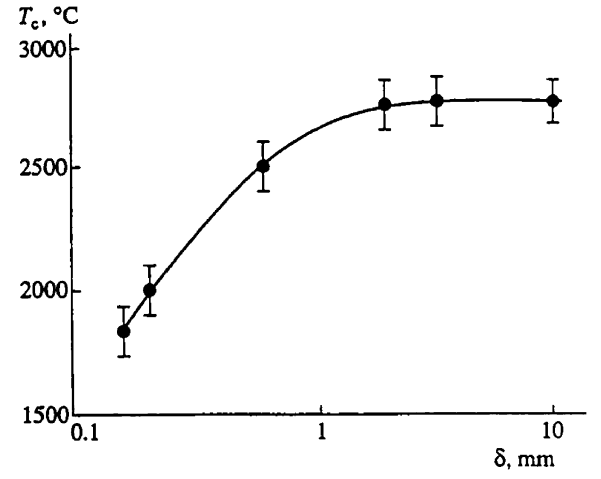

Fig. 7. Maximum temperature of combustion of Ti–B mixture as a function of thickness [17].

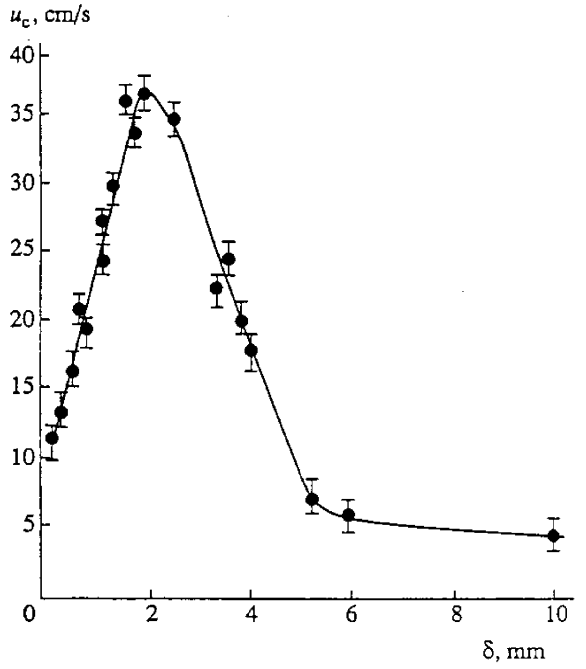

Fig. 8. Rate of combustion of Ti–B mixture clamped between plates as function of the thickness [17].

the maximum temperature rises and the combustion rate grows. This result can be attributed to the reduction of heat losses, which promotes the growth of temperature in the zone that dictates the combustion rate [17].

The size of the pellet has also an influence on the swelling of the sample. In the case of synthesis of tungsten powder from Zn and WO_3 powders use the following reactions:

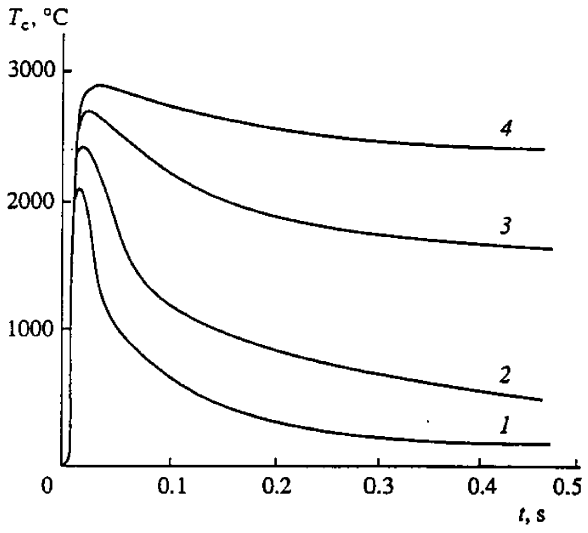

Fig. 9. Variation of the temperature profile of the combustion wave with different values of bed thickness: (1) 0.2 (2) 0.6 (3) 1.8 and (4) 3.4 mm [17].

$$WO_3 + 3Zn \rightarrow 3ZnO + W$$

The sample swelling grows from 4.9 to 14.9% as the sample diameter increases from 1.5×10^{-2} m up to 4×10^{-2} (see Fig. 10). This can be explained by the fact that Zn vapour easily leaves the combustion front through the sample surface with a decrease of the sample diameter. The tungsten particle size increased as the sample diameter increased. The radial temperature gradient which determines the over cooling rate decreases as the sample diameter increases; thus, the particle growth from lower cooling rate [11].

3.3. Evolution of gaseous species

Impurities may be present on the surface of particles in green compact and it is a source of evolution of gaseous species.

The evolution of gaseous species in the sample at high combustion temperatures can result in structural imperfections in the product as voids, or complete destruction by explosion. The rapid and large volume expansion of the adsorbed gases present on the reactant particles and entrapped gases at particle packing interstices is the principal cause of product exfoliation end even explosion. In the case of synthesis of titanium carbide the gas evolution is remarkable; the gases products during the reactions are: CO, H_2; the total quantity of evolved gases is a function of powder characteristic. The major gas produced is hydrogen; it was observed that the hydrogen originates from the water vapour adsorbed on

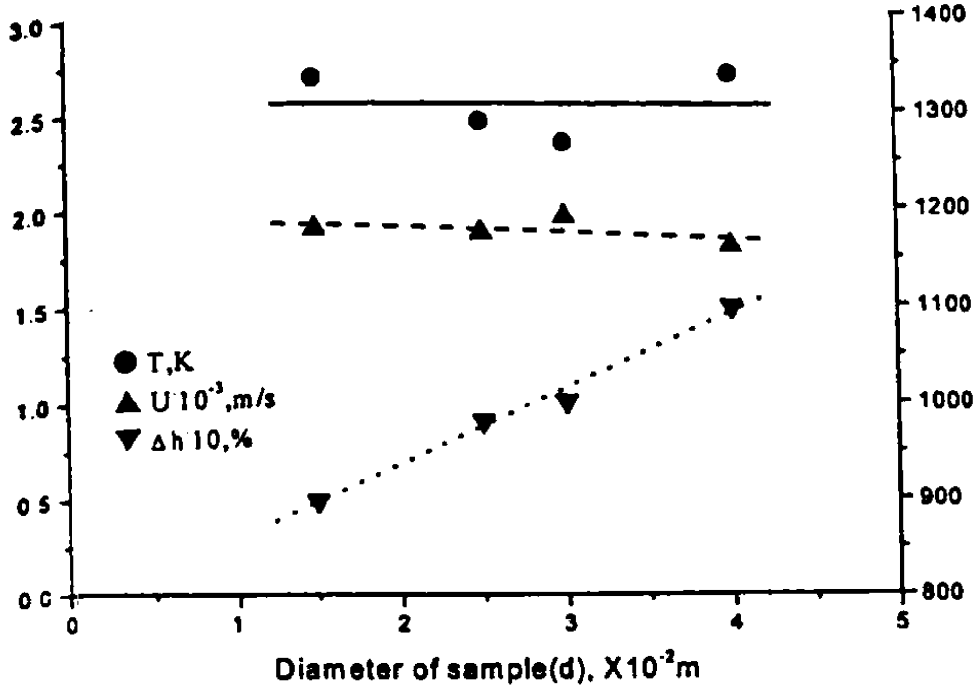

Fig. 10. Effect of green pellet diameter on the combustion parameters (where U is the combustion velocity, and Δh is the swelling [11]).

the powders (in particular on the carbon black) or from the TiH_2 present on the surface of titanium; the CO is generated by carbothermal reduction of TiO_2 present on the titanium surface [13,18].

Special interest is the problem of purification from impurity of oxygen. Considering the synthesis of TiC, the oxygen is present in two modifications: in the form of oxide film that covers the particle of the reactants and dissolved in to the particle bulk; the oxide film may take part in the reactions, more difficult is to get rid of oxygen that dissolved in metal particles but at very high temperature there is a self purification for the synthesis of TiC, and it was found that there was an increase with the increase of the combustion temperature [19].

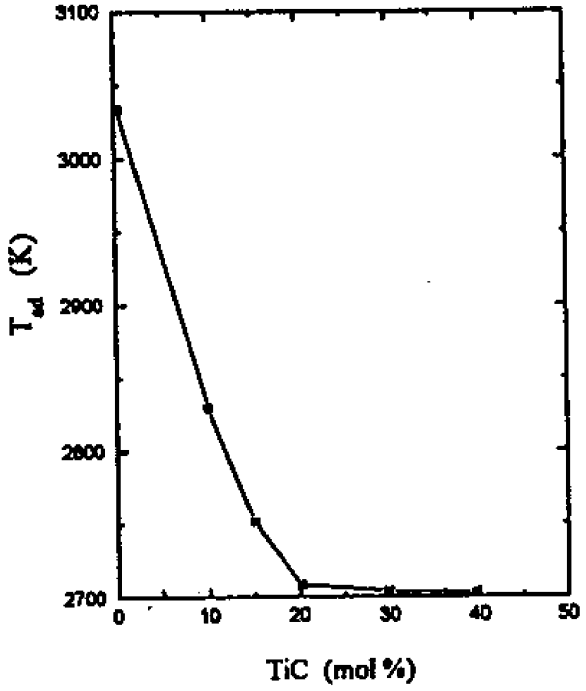

Fig. 11. Effect of addition of a diluent in the synthesis of TiC [3].

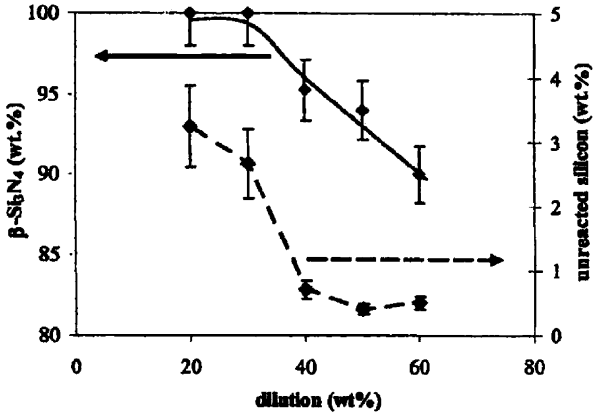

Fig. 12. β-Si_3N_4 phase (upper curve) and silicon (lower curve) contents for different dilution (80% porosity) [14].

Sample degassing and self-purification are related to the formation of a porous structure in the products, if a preliminary heat treatment of the green compact in a vacuum system is made, and the reaction carried out in vacuum, the products retain the initial shape and dimension [13,20].

3.4. Stoichiometry of the reactants

The stoichiometry of the reactants is another important process parameter. Generally the deviation from the stoichiometry results in a decrease of the adiabatic temperature, any excess of either reactants or products will normally decrease the exothermicity of the reaction with a consequent reduction of the adiabatic temperature through a reduction in the heat liberated.

The addiction of excess product as a diluent is used to control the reaction process when decreasing the adiabatic temperature and makes the reaction less violent. For example if considering the synthesis of TiC the addition of TiC as a diluent is shown in Fig. 11 [3].

In the case of the synthesis of AlN from a metallic powder of Al and nitrogen gaseous, the Al metal melts and coalesces into a pool before the beginning of the reaction, this phenomenon restricts the flow of N_2 to the reaction site. It is possible to prevent the coalescence by adding a diluent [2].

The synthesis of Si_3N_4 in nitrogen atmosphere presents high reaction speeds and, therefore, the microstructural control is difficult. Besides, the combustion temperatures are very high and silicon particles melt in the combustion front and coalesce during the reaction and inhibit complete nitridation[23]. Also this case is possible by adding a diluent.

The type of Si_3N_4 diluent (α or β) plays an important role in determining the phase composition of the final products, the data indicate that Si_3N_4 formed from the combustion reaction is primarily of the same phase as that when the diluent was added [14].

The dilution also has an effect on unreacted silicon after combustion. The unreacted silicon content, as seen in Fig. 12, also decreases in the dilution range from 20 up to 40% but it remains constant for higher dilution values. The effect of diluent content on the combustion velocity is also shown in Fig. 13.

For the samples with 60% porosity the fig. displays a maximum velocity at about 40% diluent content. The presence of this maximum value is a consequence of the melting of reactant Si. In general, from the point of view of combustion theory it is expected that as the diluent content increases, the combustion velocity decreases due to the decrease in the rate of heat generation. This trend is demonstrated in Fig. 18 by samples with diluent content within the range 40–60%. The results obtained on samples with low diluent content (<40%) are inconsistent with this behaviour. In these cases the decrease in

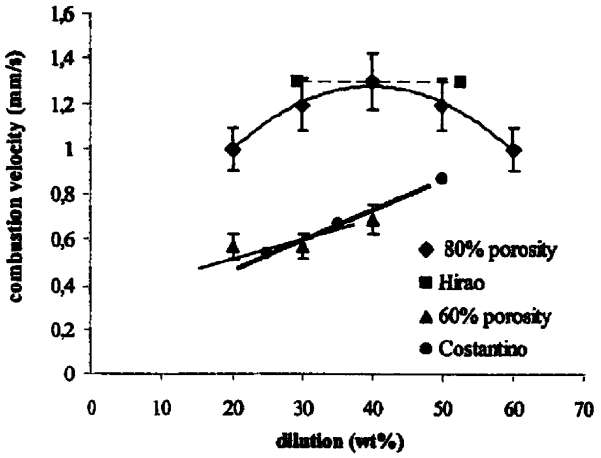

Fig. 13. Combustion velocities with 80 and 60% porosity [14].

the combustion velocity is the result of the reduction in the effective area of the reaction interface due to the melting and coalescence of reactants Si. The increase in the diluent content makes it difficult and leads to a higher reaction interface area, hence the rate of heat generation and the combustion velocity increases; as a consequence the influence of dilution on the combustion velocity depends on the percentage of diluent.

At the initial porosity of 60% the combustion was possible at 20, 30 and 40% dilution, with no effect on unreacted silicon content and a small effect on β-Si_3N_4. Samples with 50 and 60 wt.% diluent content could not be ignited. When a more powerful ignition pellet was used, a small part of the sample in the vicinity of the igniter was reacted, but self-sustained combustion did not take place. After the samples with 80% porosity, the effect of the coalescence of melted silicon particles is dominant in the range of 20–40% diluent content.

If dilution increases there are fewer silicon particles between the silicon nitride particles. Hence the distance between the Si particles grows while the coalescence effect becomes weaker. Therefore the specific surface of the reaction interface is higher and these phenomena result in an increase in combustion velocity. A further increase in diluent content, as a result for a sample with 80% porosity, show changes in the role of dilution. In this case, the main effect of dilution is the decrease in the heat generation rate which leads to on interruption of the combustion process [14].

In fact sometimes ammonium salts are added in the initial mixture (generally ammonium halides such as NH_4Cl and NH_4F) to improve the process. These salts generally sublime to relatively low temperatures producing a fluffiness effect, and improves the nitridation process, and the addition of ammonium and metals halides can promote the α-phase formation [21].

Another effect of the addition of diluent is that adding between the 10 and 20 wt.% of diluent to the reactant mixture, the degree of sintering could be decreased and the reaction product was in the form of powder and did not need to be pulverised [18].

3.5. Effect of gas pressure

The SHS gas–solid reaction can involve a different gas, for the formation of nitride, oxide and hydride; the pressure of N_2, H_2, O_2 plays an important role, but the role of the gas pressure is also important when it does not participate in the reaction.

Considering the reaction with a solid element and nitrogen, thermodynamic analysis provides information on the minimum nitrogen pressure required for the formation nitride phase, and thus gives a lower limit for the required nitrogen pressure under which the nitride is stable. For the reaction between a metal M and nitrogen: i.e.

$$M_{(solid)} + 1/2N_{2(gas)} \rightarrow MN_{(solid)}$$

The minimum nitrogen pressure p_{N2} for the spontaneous formation of the phase MN is:

$$p_{N2} = \exp\left(\frac{2\Delta G^{\circ}}{RgT}\right) \quad (13)$$

However, higher nitrogen pressures are required to make the nitridation reaction self-sustaining [1].

Another relation provides the degree of conversion, η vs the pressure of the nitrogen gas:

$$\eta = (1/S)p_{N2}\left[\frac{\pi}{1-\pi}\right]V_m/RT \quad (14)$$

where p_{N2} is the pressure of N_2(g), π is the initial porosity of the sample, V_m is the molar volume of the metal, S is the stoichiometry ratio of the nitride (i.e. number of moles of N_2 per mole of metal in the reaction), R and T have their usual meanings.

A plot of log p_{N2} versus η for selected nitrides is shown in Fig. 14. The fig. shows that, for example, complete conversion of Zr to ZrN with nitrogen already existing in the pore of a compact with $\pi = 0.7$ requires p_{N2} to be about 2×10^{-3} atm. Higher pressures would be required for the formation of the other nitrides. The equation can be used to demonstrate the susceptibility of the synthesis of various nitrides to the problem of permeation [2].

In the case of the formation of hydrides, in particular, considering the example of yttrium with hydrogen, forming hydrides with MeH_3 and MeH_3 compositions, the yttrium readily ignites in hydrogen at $P_{H2} = 1$ atm. The combustion product is yttrium hydride. The influence of hydrogen pressure is considerable, particularly on the metal of group IV. With the increase of pressure, the temperature and the rate of combustion grow [22].

In the case of the interaction of niobium with hydrogen it was found that the combustion occurs in auto-oscillation (pulsation) regime. Fig. 15 shows the thermograms obtained at combustion of niobium at different hydrogen pressures. The dependence of niobium combustion velocity on the hydrogen pressure is shown in Fig. 16. It can be noticed that with an increase in pressure up to 50 atm the combustion rate increases drastically. Fig. 17 shows the dependence of the combustion temperature and hydrogen content on pressure in the Nb–H system, it is also illustrates two regions of niobium hydrides formation. In the region I at relatively low hydrogen pressure the combustion proceeds toward the formation of mono-hydride of niobium (β-phase); the combustion temperature being between 450 and 600° C. In region II with increasing hydrogen pressure niobium dihydride $NbH_{1.84}$ was formed. However together with dihydride fcc phase, the orthorhombic monohydride phase is always formed. It has been shown that the combustion regularities (T_{comb}, U_{comb}) and hydrogen content depend on the Nb powder dispersion [23].

In the synthesis of $Ni_{0.35}Zn_{0.65}Fe_2O_4$ ferrite powders, the oxygen reactant is involved in the process and determines the process parameters T_c and U_c (combustion temperature and combustion wave velocity) with the increase of oxygen pressure; T_C and U_c increase obviously. During the SHS process, oxygen exists in three kinetic potential barriers, i.e. the penetration of oxygen from the environment into the combustion zone; the oxidation of iron and the infiltration of oxygen through the melting product layer. In the SHS reaction,

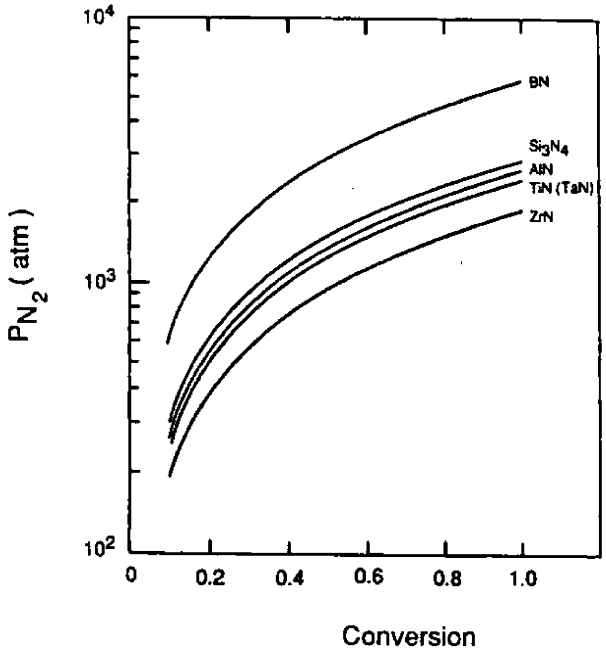

Fig. 14. The dependence of degree of conversion to nitrides on p_{N2} for selected elements [2].

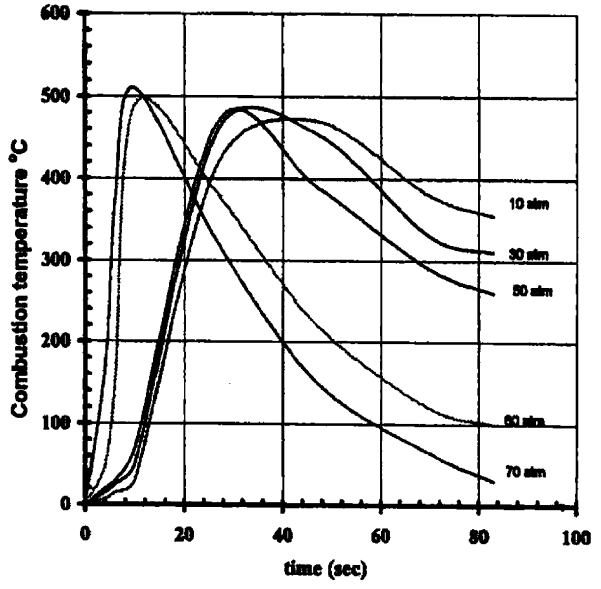

Fig. 15. The thermograms recorded at combustion of niobium at different hydrogen pressures [23].

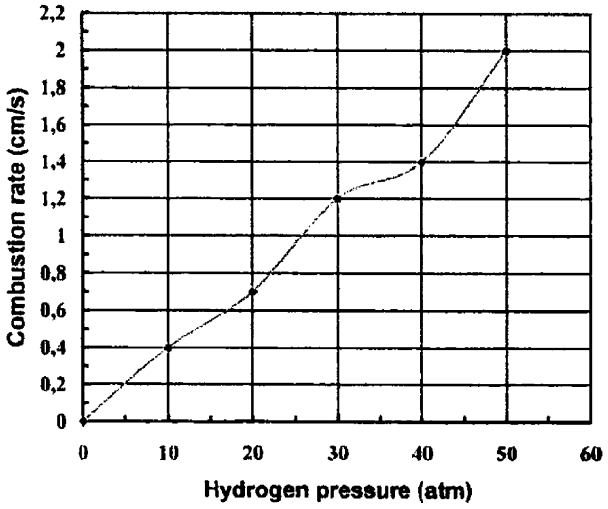

Fig. 16. The dependence of niobium combustion velocity on the hydrogen pressure [23].

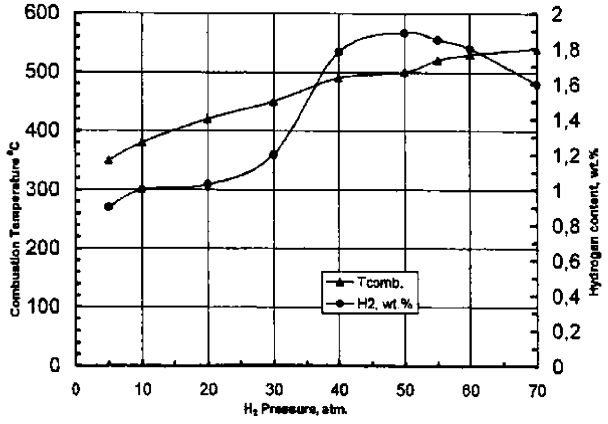

Fig. 17. The dependence of combustion temperature and hydrogen content in products on pressure in Nb–H system [23].

carried out under the low oxygen pressure, the ferritization degree of the combustion products will be low. This is caused by the shortage of oxygen and the lack of permeability. High oxygen pressure enhances the oxidation reaction of iron, increasing the combustion temperature and combustion wave velocity during the combustion reaction, due to the sufficient oxygen content and its proximity between particles [12].

But the gas pressure influences the reaction parameters also if the gas is not involved in the reaction. The combustion velocity of most SHS systems usually increases when increasing the external pressure and remain constant once a certain pressure level are reached. The augmentation of combustion velocity is concerned with the suppression of the expansion process during sample burning and the improvement of thermal contact between particles. From this point of view the system $3SiO_2/4Al/3C$ is not an exception, (see Fig. 18) where the combustion temperature and front velocity are reported as a function of working pressure and gaseous atmosphere. In fact, as the pressure is increased the

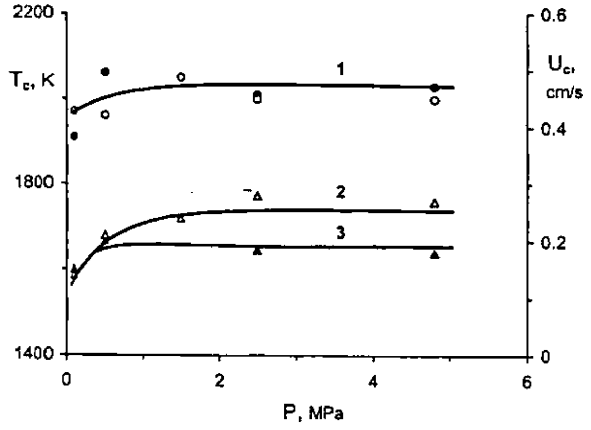

Fig. 18. Influence of gas pressure on combustion temperature and velocity for the system 3 SiO_2/4Al/3C 4% Teflon: 1, T_c (○, in nitrogen; •, in argon medium); 2, 3 U_c (2 in nitrogen; 3 in argon medium) [24].

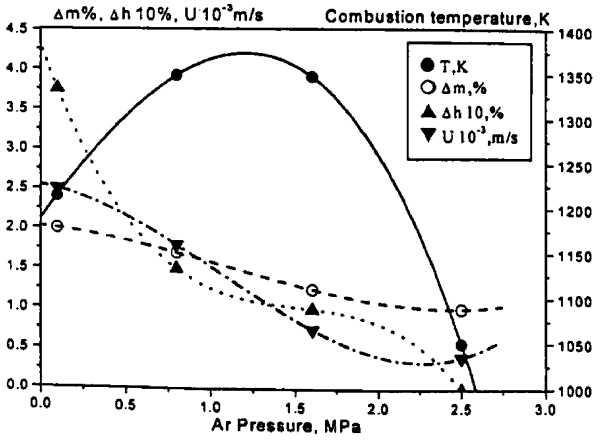

Fig. 19. Effect of Ar pressure on combustion parameters [11].

combustion velocity does the same, reaching a constant value. When $P \geqslant 0.5$ MPa the combustion velocity in nitrogen is appreciably higher than argon, while the combustion temperature is practically the same. This finding demonstrates that at high pressure levels the gaseous nitrogen certainly participates in the reaction [24].

In the synthesis of ZnO/W (Fig. 19) considering the effect of argon pressure on the combustion parameters if the pressure increases from 0.1 up to 0.8 MPa the combustion temperature increased and then remains constant up to the pressure of 1.6 MPa. With argon pressure up to 2.5 MPa the combustion temperature decreases. In the case of further pressure increase, the combustion flame did not self-sustain. The combustion velocity U, sample weight change Δm and elongation decreased as the Ar pressure increased, and the combustion was observed in a spin mode. It was demonstrated that the evaporation of the metal vapour is suppressed by Ar pressure. Hence, the increases of Ar pressure resulted in the decreases of the evaporation of easily volatile components, Zn. However further increases of the Ar pressure resulted in the decreases of the combustion temperatures and finally the self-sustained combustion could not be achieved. There may be a possible explanation on this phenomena, one is that the heat removal from the sample surface becomes higher with the Ar pressure increase; another one is that the vaporised Zn acts as a heat transportation medium [11].

3.6. Ignition

There are many different techniques to ignite SHS reactions. The usually ignitor is composed of a tungsten wire that became hot through an electric discharge and ignites the mixture directly. If the reaction needs, it is possible to add a mixture of various components that produce an exothermic reaction to ignite the sample. In order to standardise the conditions of the ignition for each reaction it is possible to use a radiant flux, this type of ignition is composed of a radiation source, a reflector used to converge the reaction and a shutter for the control of the amount of the radiation.

Another way to ignite the sample is to use a laser; in this case it is possible to obtain a very high heat flux densities.

The chemical ignition is made by putting in contact with the green powders, a reactive gaseous or a liquid reagent on account of the evolution of sufficient heat at the contact surface.

Combustion synthesis reactions can also be ignited using microwave energy, in this way the SHS reactions initiate in the centre of the green pellets and propagates outwards towards the surface.

Finally it is possible to heat the entire sample at constant rate to obtain a simultaneous combustion [3].

4. Other types of SHS processes

It is clear, reading SHS literature, that this process is very efficient only for the reactions that are high exothermic. If the reactions are not so exothermic the front do not propagate, this is for example the case of a large number of single-phase and composite materials both ceramic and intermetallics compounds, but sometimes these compounds are very interesting from a technological point of view. In addition, SHS reactions are limited by kinetic considerations. These include the rate of the reactions and the rate of heat transfer ahead of the reaction front. The latter is governed by the effective thermal conductivity of the product phases.

The need for activation stems from the thermodynamic and kinetic limitation of SHS. This can be seen through an examination of the governing Fourier adiabatic heat balance equation with a heat source (see Section 4). Q Represents the thermodynamic limitation, while the kinetic limitation is represented by the rate of the reaction and by the thermal conductivity. The rate of the reaction is governed by either chemical kinetics or mass-transport kinetics. The latter is operative in cases where the diffusion through product layers is rate controlling. The case of the thermal conductivity is more complex since higher k values mean lower temperature gradients and vice versa. Thus the first term on the left-hand side of the equation is low at very low and very high thermal conductivity.

The conclusion of all of this observation is the inability to establish a self-sustaining front in the case of: (a) low enthalpy reactions, (b) high thermal conductivity reactant mixtures, (c) in some kinetically controlled high enthalpy reactions [25].

So many researchers in different country have developed a new SHS process coupling with others techniques that are able to sustain the reaction, furnishing supplementary energy for the propagation of the combustion wave.

4.1. Field activated SHS (FACS)

Recently a new method has been developed to activated a sluggish SHS process and thus overcome both thermodynamic and kinetic limitation. In particular the approach involves in the imposition of a voltage across the reactant compact and activation of a heating coil as an ignition source as shown in Fig. 20. In general the imposition of a field or an ignition source alone does not produce self-propagating waves. However, simultaneously imposed these conditions produced such reaction waves [25].

The effect of an electric field on reactions can be multi-faceted; the field (in reality a current) can have a thermal effect (joule heating), a mass transport effect (electro-migration) or a more complex effect arising from reported plasma creation in the powder compact. Modelling studies based on the assumption that the main effect is Joule heating [26].

With the application of an electric field it is possible to synthesise very interesting composites, for example AlN–SiC, the common method for synthesis or this solid solution is heat powder mixture of AlN and SiC at above 2100 °C for several hours, using field-activation was made with the following reactions:

$$Si_3N_4 + 4\ Al + 3\ C \rightarrow 4AlN + 3\ SiC$$

This reaction is highly exothermic, but no self-sustaining reaction can be established without field-activation. However on SHS reactions does occur unless the applied field is $\geqslant 8$ V/cm. At 8 V/cm, the reaction is incomplete. At field between 8 and 25 V/cm the reaction is complete with the product containing AlN and SiC [25].

The effects of the field on the rate of the reaction are shown in Fig. 21 for the synthesis of SiC from the elements, the wave velocity is plotted as a function of the field. The fig. shows three regions, relative to the strength of the applied field. At low fields $\leqslant 6$ V/cm no SHS reactions takes place, but above this threshold value the rate of self-sustaining reactions increases approximately linearly with field strength. At relatively high field $\geqslant 21$ V/cm, no ignition source is required and the reaction occurs through Joule heating of the reactants by applied field. In this case no self-sustaining wave is present and the reaction occurs simultaneously throughout the sample. Examination of the electric parameters, such as voltage and current, during wave

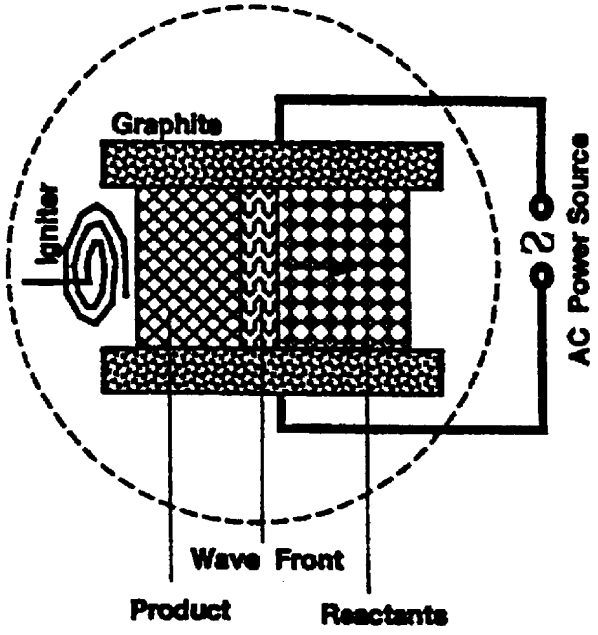

Fig. 20. Schematic representation of the field-activated combustion process [26].

propagation is shown in Fig. 22. As the wave begins to propagate (indicate by "S") the voltage drops initially and then remains relatively constant until the wave reaches the end of the sample (indicated by "E"). The behaviour of the current is consistent with that of the voltage, so is the behaviour of the calculated resistance [25].

The constancy of three parameters during wave propagation means that the current is primarily confined to the narrow reaction zone. The localization of the current to the reaction zone is not unique to SiC but is typical of all reaction systems whose reaction products

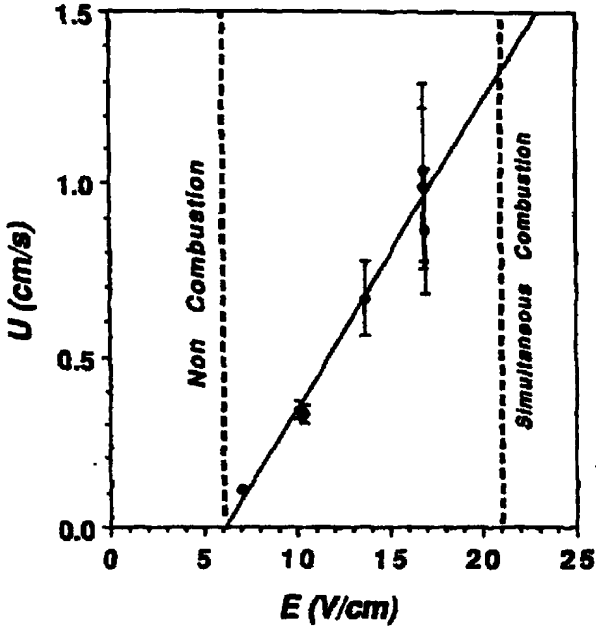

Fig. 21. The effect of field on velocity of wave propagation in the synthesis of SiC [25].

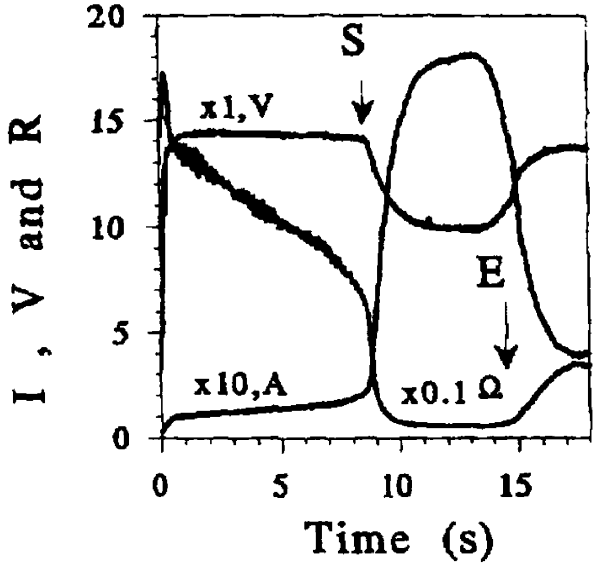

Fig. 22. Current, voltage and resistance variations during wave propagation in the synthesis of SiC [25].

are relatively non conducting [25]. Also in the synthesis of silicon-containing materials, it was concluded that the current is primarily localized in the combustion zone and that circumstance is aided by higher conductivity in this region due to the melting of Si [27]. It was observed that the degree of activation depends strongly on the electrical conductivity of the product phase [26]. If the products are conducting then the contribution of the electric heat to the reaction zone decreases as a function of distance travelled by the wave. The velocity of the wave is anticipated to decrease with the possibility of extinction of the combustion front before it reaches the end of the sample. Considering the synthesis of Nb_5Si_3 under the influence of a field of 10.7 V/cm the wave traversed the entire sample; but at lower fields (e.g. 7.8 V/cm) the continuous wave propagation changed to a spin mode of reaction advancement before reaching the end of the sample [25].

In the synthesis of composites WSi_2–Nb for all values of the applied field the Nb-free system had the highest current; and for any given field, the current decreases systematically with increasing x value (vol.% of Nb). This observation would seem contrary to expectations that a higher metal content should lead to higher conductivity and hence higher current. Thus the addition of Nb (which remains in the solid state) decreases the volume fraction of the molten phase and hence the effective conductivity. Considering the synthesis of WSi_2–ZrO_2 the ZrO_2 additive, was qualitatively similar than the case of Nb addition and the proposed explanation, related to the role of liquid phase is believed to be equally valid [27]. The wave velocity increases with increase in the applied field (in the synthesis of WSi_2–Nb) for all Nb concentration; moreover for any given applied field the velocity decreases with an increase in the level of Nb additive. This is consistent with the effect of Nb addition on the maximum current. A decrease in the current represents a decrease in the degree of electrical activation and hence a decrease in velocity. The addition of ZrO_2 is likewise similar [27].

The modelling study is based on the premise that the imposition of the electric field is equivalent to the addition of another heat source. Using the Fourier equation and accounting for radiative heat loss, the modified equation becomes:

$$\rho C_p \frac{\partial T}{\partial t} = \kappa\left(\frac{\partial^2 T}{\partial x^2} + \frac{\partial^2 T}{\partial y^2}\right) + \rho Q \frac{\partial \eta}{\partial t} + \sigma E^2 - \frac{O_s}{W} \times \left(T^4 - T_0^4\right) \quad (15)$$

where σ is the electrical conductivity, E is the electric field, σ_s is the Stefan–Boltzmann constant, T_0 is the ambient temperature, W is the sample thickness. The third term on the right-hand side of the equation is the rate of heat imported to the sample from the electric field while the second term is the rate of chemical heat evolution [25].

The effect of the green density on the measured electric parameters (current, voltage and power) during wave propagation is show in Fig. 23 (a)–(c) respectively. Fig. 23(a) shows the changes in the current profiles at constant applied voltage for the sample with relative densities of 60, 65 and 70%. As the density increases the on set of the rapid increase in the current takes place at an earlier time. The extension of the current profiles, for the denser samples to longer times is a consequence of decrease in velocity with increasing relative density.

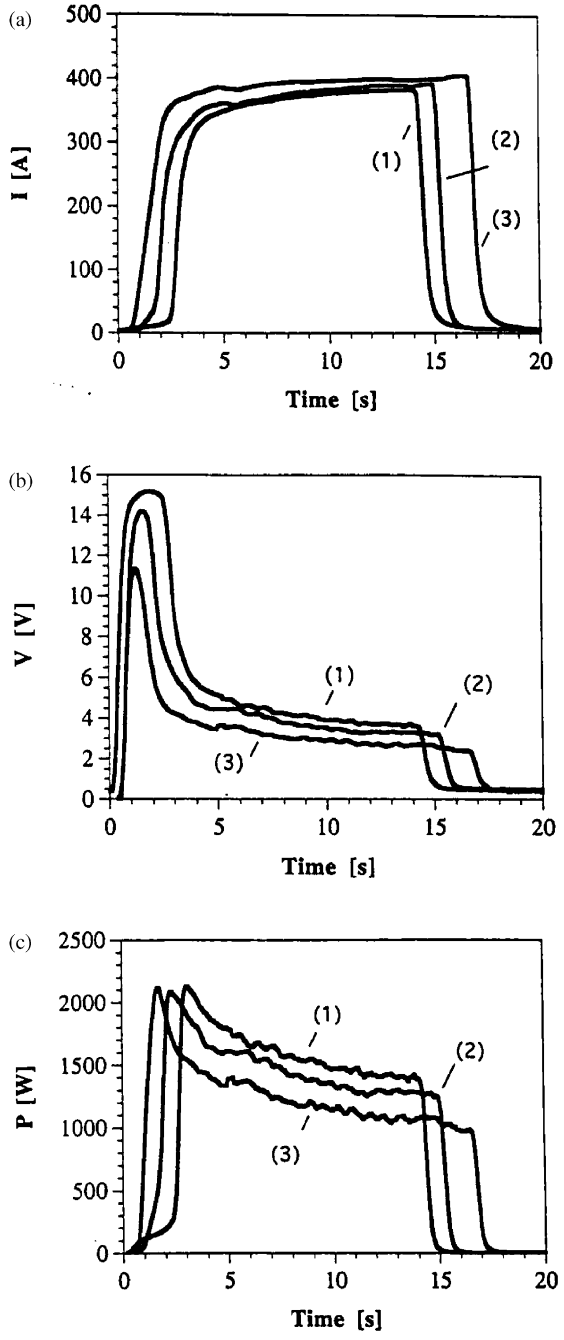

Fig. 23. Effect of relative density on (a) current (b) voltage and (c) electric powder during the synthesis of Ti_3Al (E = 10.7 V/cm): (1) 60%, (2) 65%, (3) 75% density [26].

The effect of the density on the voltage profiles shows a corresponding behaviour [Fig. 23(b)]. The maximum voltage decreases as the relative density increases. The corresponding electrical-power profiles, which are equivalent to the rate of heat release to reaching samples during synthesis and are the product of the instantaneous voltage and current values in the three previously examined cases, are shown in Fig. 3(c). For high-density samples, the maximum power value is reached immediately after the field is applied. In all cases the electric power decreases during wave propagation. With decreasing pellet density, the power profiles exhibits his maximum at increasing times and shows a less-sharp decrease afterward as seen in Fig. 23(c) [26].

It also interesting that is possible by this method to obtain the products without the undesired phases and using a crystalline reactant that normally in the same case is not possible, for example the synthesis of TiB_2–$TiAl_3$. Using amorphous boron reactant composites with molar ratio $TiAl_3/TiB_2 = x$ with $x \leqslant 2$ can be synthesised without the application of a field. However, composites with $0 \leqslant x \leqslant 5.0$ can be synthesised in the presence of field. In both cases the products contained the desired $TiAl_3$ and TiB_2 phases with minor amounts of Ti_5Al_{11}. Considering molar ratio $x = 1$ it is possible to use a crystalline boron powders for the reaction only with the application of a field (in this case of 18 V/cm), the mode of wave propagation is: steady-state for the powders with particle size of boron $\leqslant 30$ μm, for higher value in the pulsating mode. The products obtained are the same at those obtained with amorphous boron [28].

4.2. Mechanically activated SHS (MRS and MASHS)

Another way to increase the reactivity of the green powders is the process that combines simultaneously or successively ball milling (MA) and an SHS reaction. However, there has been an important improvement in these two methods of synthesis, in the same time. But it was only in the early 1990s that a strong increase in the number of papers related this combination of techniques.

They can be classified as follow: (1) Mechanically-induced Self-propagating Reactions (MRS) for which as SHS reaction occurs during milling inside the ball mill after same activation time, when the powder reaches a well-defined critical state. (2) Mechanically Activated Self-propagating High-temperature Synthesis (MASHS) which consists of a short duration high-energy ball milling step followed by SHS.

Indeed, the mechanically activated mixtures were found to be composed of particles containing a nano-distribution of the element component without the formation of

mechanically induced product phases. The effects of the milling conditions on the grain sizes and on the residual stresses were reported to modify the phase transformation kinetics in the final self-sustaining synthesis. Whatever the nature of mixture components, the milling process, which causes the intimate mixing of particles on a nanoscale, leads to the reduction in the crystallite size and accumulation of defects in powder particles, which introduce an additional energy to the reactant system in the form of interfacial energy and strain energy. This effectively lowers the activation barriers for reactions. In addition, in most cases the rate of refinement of the internal structure (i.e., particle size, crystallite size, lamellar spacing, etc.) is roughly logarithmic with the processing time or with the ball-to powder ratio. This variation is described in Fig. 24.

Indeed, in a few minutes to an hour, the lamellar spacing usually becomes small and the crystallite size is refined to nanometer dimensions.

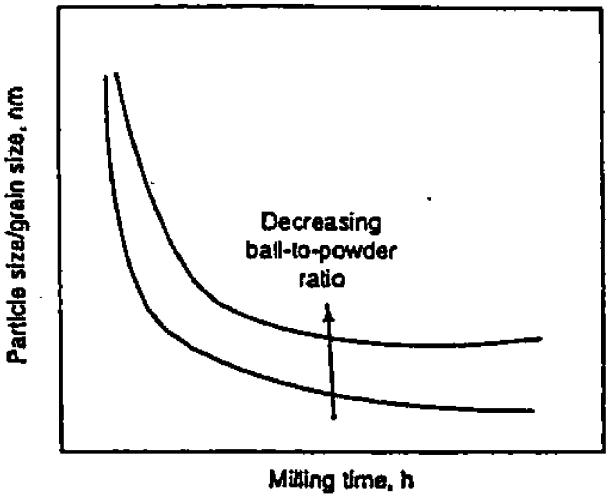

Fig. 24. Refinement of particles and grain size with milling time. Rate of refinement increases with higher milling energy, ball-to-powder weight ratio, lower temperature, etc. [29].

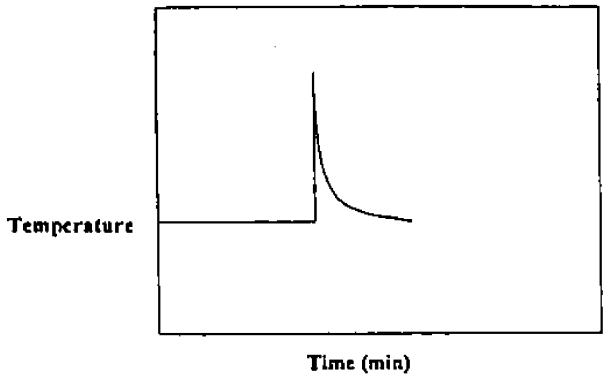

Fig. 25. Temperature of milling container during mechanochemical reduction of magnetite with zirconium [29].

Moreover, the presence of a variety of crystal defects (i.e. dislocations, vacancies, staking faults, grain boundaries, etc.) enhances the diffusivity of solute elements into the matrix. Further, the refined microstructural features decrease the diffusion distances. In addition, the slight rise in temperature during milling activates the diffusion behaviour, and consequently, true alloying takes place among the constituent elements.

4.2.1. MRS

The latter type of reactions requires a critical milling time or critical injected powder for the combustion reaction to be ignited inside the ball milling. If the temperature of the vial is monitored the milling process, the temperature initially increases slowly with time. After a critical value, the temperature increases abruptly, suggesting that the ignition has occurred (Fig. 25).

The time at which the sudden increase in temperature occurs is referred to as ignition and from hereon as t_{ig}. For certain highly exothermic reactant systems, however, spontaneous compound formation can occur by a mechanically induced Self-propagating High-temperature Synthesis. The occurrence of MRS during mechanical alloying is usually preceded by an induction period, the length of which depends on the milling condition and the exothemicity of the reactant system.

Once a small powder mixture reacts during milling, the heat, which has been liberated by the exothermic, propagates and ignites the unreacted portion until the bulk of the elemental powder mixture is converted into the product.

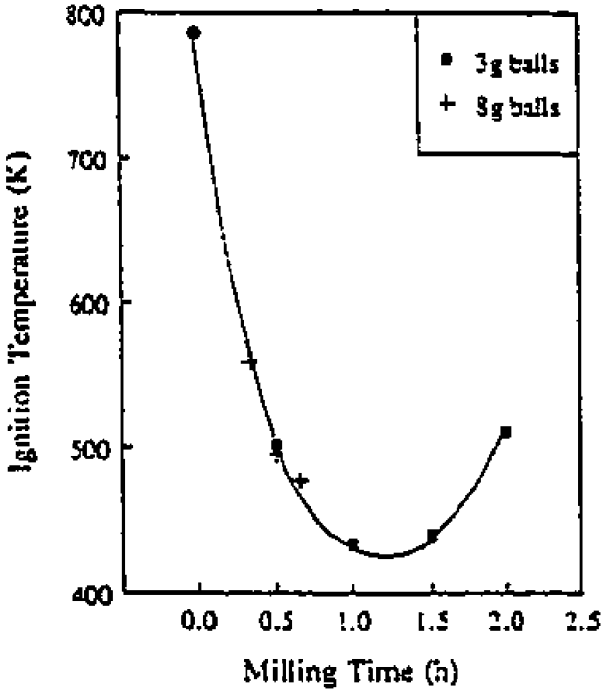

Fig. 26. Variation in ignition temperature with milling time [29].

The large enthalpy changes associated with the chemical reactions have been identified as being responsible for the occurrence of the combustion reaction. If the temperature generated during the milling process (due to ball-to-ball and ball-to-powder collision), T_c, is higher than T_{ig}, then the combustion reaction can occur. T_{ig} Is a function of enthalpy change and micro structural parameters.

Since the MA process refines the particle size, T_{ig} decreases with the milling time as shown in Fig. 26, in the case of reaction between CuO and Fe.

However, with increasing milling time T_c increases and reaches a steady state. The time at which T_{ig} and T_c intersect is critical milling time t_{ig} at which the combustion would have occurred. It may also be interpreted that during t_{ig}, intermixing of the particles, particle refinement and accumulation of lattice defects occur and these appear to favour the combustion reaction. (Fig. 27).

However, it has been noted that many of these reactions are not directly completed: instead, intermediate phases are formed.

4.2.2. MASHS

The use of mechanical activation as a precursor to SHS also results in the formation of nanostructured materials. In MASHS, the elemental powder mixture is milled for a short time at a given frequency and impact energy, and then it is used as a reactant in the SHS process. Due to the typically products they have been shown to be nanostructured. Moreover, it was necessary for the mechanical activation step to initiate a combustion front in the case of a thermodynamically non-favourable system and to modify the thermal parameters of the combustion front in other cases.

Although MASHS has great potential, this process induces the formation of porous end products containing 40–50% of porosity. Mechanical activation can multiply the combustion front velocity by a factor of three compared to the classical value obtained under the same ignition condition. Finally, high-energy ball milling treatment allows the control of the formation of pure and nanometric powders by fixing the reactant powder microstructure. In fact, mechanical activation would promote the number of potential nucleation sites and produce finer crystallites.

Consequently, crystallite growth is limited by lower temperature and large numbers of grains are formed at the same time. Normal reaction rates in SHS are considered to be of the order of 10 mm/s. Propagation rates of the order of 40 mm/s were measured for alloyed powders in same cases. The enhancing influence of MA time on the SHS propagation rate (Fig. 28) was fairly linear for 200 rpm alloying up to 5 h of milling. After 6 h, the propagation rate started to decrease rapidly. Powders milled for 7 h or more at 200 rpm did not ignite at all. When 160 rpm milling was used, the ignition behaviour had the same tendency but the influence was much slower [28].

4.3. SHS coupled gas-transport

The activation through gas phase diffusion transport augments the solid-phase diffusion transport that is required for sustain propagation of combustion wave. Even small quantities of gas can have a significant impact on SHS combustion, leading to pronounced changes in burning velocity, temperature, product elongation, and reactants-to products conversion efficiency. The presence of gas transport agents is particularly important in the systems were the adiabatic flame

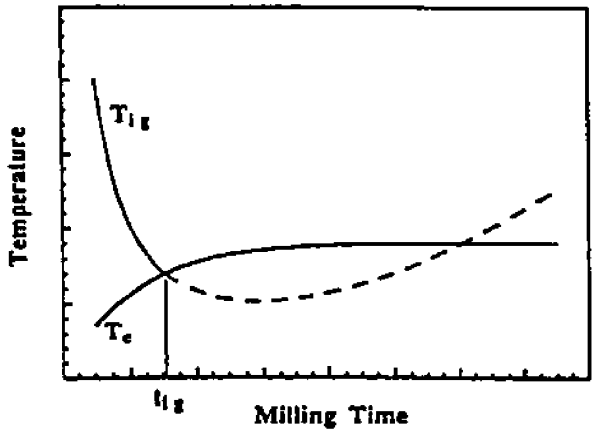

Fig. 27. Schematic representation of variation of T_{ig} and T_c with milling time. The point of intersection of t_{ig} represents the minimum ignition time [29].

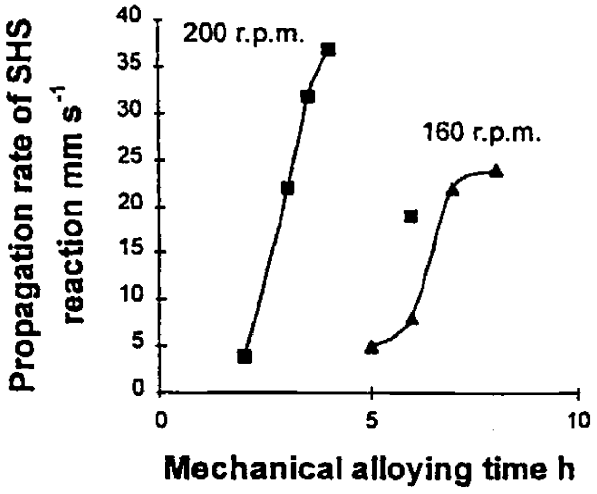

Fig. 28. Propagation rate of SHS reactions as function of MA in the Ni_3Si system at two milling intensities (rpm of the planetary ball mill) [29].

temperature is below the melting point temperatures of reactants, products, and intermediate species.

Considering the reaction:

$$Ta + C \rightarrow TaC$$

iodine (I_2) vapour and carbon dioxide (CO_2) were chosen as the gas transport agents.

Solid-phase iodine has been shown to be effective in influencing many macroscopic characteristics in Ta/C combustion systems, CO_2 has been proposed as an intermediate formed when trace oxide impurities are present in the reactant powders and carbon is used as one of the reactants.

The combustion chamber is shown in Fig. 29. Iodine was sublimed from crystal powder form and the vapour was directed into the combustion chamber. The Ta/C system was very sensitive to the presence or absence of a gas transport agent. Ignition of the samples could not be achieved without a minimum or critical mole of fraction of gas transport agent present in the chamber. In the gas-assisted SHS systems both solid-phase diffusion transport are present.

The transport of metals by halogen species is well known. Fig. 30 includes the cycle proposed. TaI_5 is produced via: $Ta_{(s)} + 51/2\ I_{2(g)} \rightarrow TaI_{5(g)}$ at low temperatures, and then tantalum condensed by reverse reaction at high temperature. In the I_2/Ta the iodine transport breaks the tantalum particles into smaller components, which should result in higher specific surface areas than if carbon simply diffused in the existing tantalum particles.

The CO_2/Ta/C transport system is more complicated than the iodine system, involving multiple steps and chemical reactions as seen in Fig. 31. The presence of the transport agent enhances the conversion of reactants

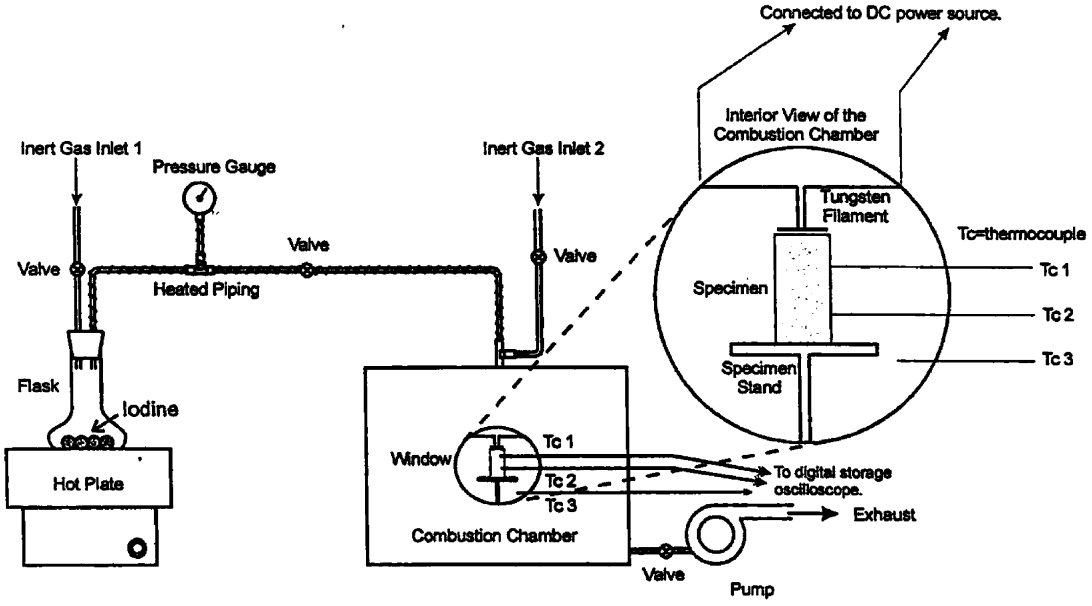

Fig. 29. Experimental schema of the combustion chamber [30].

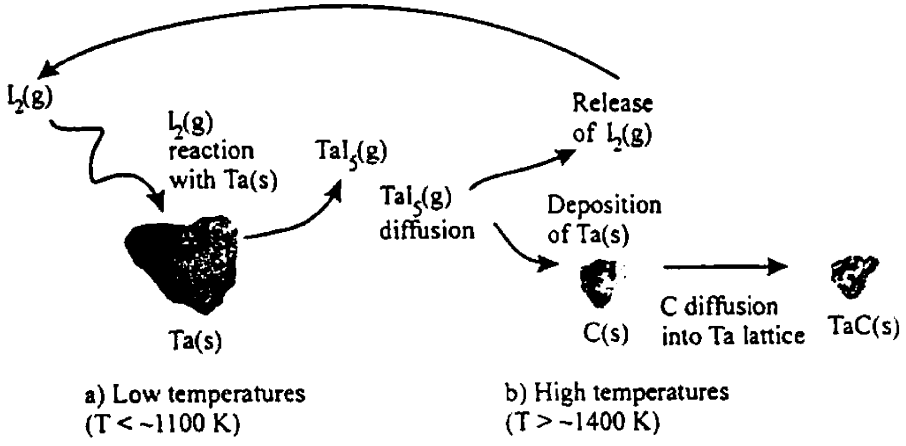

Fig. 30. Schema of proposed transport mechanism in the I_2/Ta/C system [30].

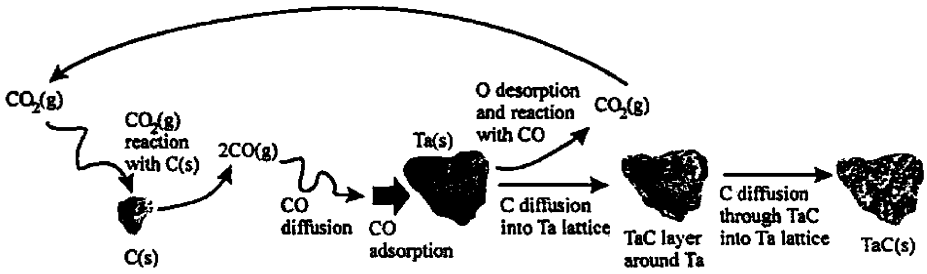

Fig. 31. Schema of proposed transport mechanism in the CO_2/Ta/C system [30].

Table 2
Industrial parameters of SHS, FS, PCS synthesis processes [31,32]

Parameter	SHS	FS	PCS
Consumption of the raw materials:			
Aluminum/kg (kg^{-1})	0.7	0.9	1.5
Nitrogen/m^3 (kg^{-1})	0.9	1.65	12.3
Consumption of electric energy/kWh kg^{-1}	0.5	31	150
Labor consumptions (rel. unit)	1	1.4	3.5
Number of technological stage	8	18	5
Effectiveness (kg h^{-1})	4.0	1.0	0.75
Time of technological stage/h	0.6	2.5	0.5
Net cost powder (rel. unit)	1	2	4

to products and results in higher tantalum carbide stoichiometry, although CO_2 is not as effective as iodine for most conditions.

Particle size effects, in catalytically assisted SHS, are due to the surface contact area between particles and corresponding void fraction samples. In the combustion synthesis where the gas transport is minimal, smaller reactants generally lead to increased contact area between reactants and therefore higher reaction rates. In this case the specimens had larger void fractions with less contact area between particles. The results from the iodine experiment indicate that a critical pore size may exist for the iodine-assisted SHS system with different transport mechanisms, limiting the conversion process for systems above or below this critical pore size. In iodine systems with pore sizes below the critical pore size, gas-phase transport is more rapid and solid diffusion may become the limiting transport process [30].

5. Economical and environmental impact

The economical effectiveness of SHS is evident when we consider the production of some nitrides from the same raw materials using furnace technologies.

The technological parameters of three types of industry that produce aluminium nitride powders in three different ways: SHS, furnace (FS) and plasmochemical (PCS) are compared in Table 2. As can be seen the SHS technology exceeds alternative process by almost parameters.

The calculation of the complete power saving in the synthesis of titanium carbide powders: by the furnace method ($TiO_2 + 3C \rightarrow TiC + 2\ CO$) requires 35 kWh kg^{-1}; similar parameters for two SHS methods are 2–3 kWh kg^{-1} from elemental ($Ti + C \rightarrow TiC$) and magnesium-thermal ($TiO_2 + 2Mg + C \rightarrow TiC + 2\ MgO$) methods, the energy consummations in the traditional technology are related to the furnace heating but in the SHS technology they are associated with reprocessing of the product after combustion (in the first case mechanical treatment and in the second case chemical and metallurgical treatments). Taking into account that energy consumptions for the preparation of metal used in the SHS technology are equal to 11 kW kg^{-1} for Ti and 16 kW kg^{-1} for Mg. It follows from elementary calculations that the SHS technology is energy saving even taking into account the additional consumptions of electric energy for the preparation of the raw materials. The saving in electric energy is 24 kWh kg^{-1}, for SHS from the elements and 19 kWh kg^{-1}, for the magnesium-thermal method [31].

Advantages of SHS are not limited only to the economical impact. Recently a synthesis was developed that was interesting from an environmental point of view.

Self-propagating reactions of thermite type have been proposed in the literature to address an important environmental problem, i.e. the fixation of high-level radioactive wastes. The proposed process consists of reducing the volume of radioactive liquid wastes and fixing products into a highly insoluble polysilicate structure, by means of appropriate thermite reactions.

Silicon, iron oxide and silica are used to prepare the thermite mixture and to provide the desired reaction rate and final products composition. The process is based on the use of the following exothermic thermite reaction:

$$4\ Fe_2O_3 + 3\ Si \rightarrow 3Fe_2SiO_4 + 2\ Fe$$

which gives rise to the formation of polysilicate structure to incorporate the wastes. An alternative process consist of converting all salts in sulphate prior to fixation, using this reaction:

$$4\ Al_2(SO_4)_3 + 9\ Si \rightarrow 2Al_2O_3 + 9\ SiO_2 + 6\ S$$

A different process based on combustion reactions to prepare ceramic oxide materials like perovskite ($CaTiO_3$) zirconolite ($CaZrTi_2O_7$), hollandite ($Ba_{1.23}Al_{2.46}Ti_{5.54}O_{16}$) and sphene ($CaTiSiO_5$) which can be used for nuclear waste immobilisation, in fact, these oxides are characterised by the presence of cavities and a vacant interlayer in their structures so that they are capable of incorporating radioactive cations.

Highly toxic solid wastes from electrolytic zinc plants, known as jarosite or goethite depending upon the treatment used for iron removal, are currently obtained. Recently a process of treating and recycling of goethite wastes based upon SHS thermite reaction was proposed. In particular, taking advantage of the relatively high content of iron oxide in the wastes, the following thermite reactions were exploited:

$$2\ Fe_2O_3 + 3\ Si \rightarrow 3SiO_2 + 4\ Fe$$

$$Fe_2O_3 + 2\ Al \rightarrow Al_2O_3 + 2Fe$$

$$Fe_2O_3 + 3\ Mg \rightarrow 3MgO + 2\ Fe$$

$$Fe_2O_3 + 3\ Ca \rightarrow 3CaO + 2\ Fe$$

It was found that by blending this waste with a suitable amount of reducing agents as well as ferric oxide, according to reactions and igniting the resulting mixture a combustion wave rapidly travels through the mixture without requiring additional energy.

Organo-chlorine pesticides, polychloric biphenyls, dibenzofurans, dioxin, etc.. are highly resistant to oxidative degradation and dangerous emissions are possible in conventional incinerator technologies. SHS reactions can also be used to degrade chlorinated aromatics. Reactants were mixed according the following reactions:

$$3\ CaH_2 + C_6Cl_2 \rightarrow 3CaCl_2 + 6\ C + 3H_2$$

$$6\ CaH_2 + C_6Cl_2 \rightarrow 6CaHCl + 6\ C + 3H_2$$

A new recycling process based on the SHS nitriding combustion of silicon sludge, from semiconductor industries and aluminium drass, from aluminium foundries both to obtain silicon based ceramics. The process treatment of silicon sludge is based on the combination of silicon with nitrogen to form Si_3N_4 according to the following exothermic reaction:

$$3\ Si + 2\ N_2 \rightarrow Si_3N_4$$

However, the composition of silicon sludge rich in Si of 26 wt.%, the silicon content is too low to make the nitridation by SHS. To overcome this problem, reclaimed Si and Al powders produced by silicon and aluminium industries were added. The other SHS recycling processes in literature, which makes use of aluminium dross, is based on the nitridation of aluminium according with the following reaction [33].

$$2\ Al + N_2 \rightarrow 2AlN$$

Traditional vehicle exhaust catalysts are made of a small percentage of noble metals such as Pt or Pd dispersed on a high surface area carrier made of alumina supported on cordierite with honeycomb geometry. This is a complicated method of production considering also the high cost and rarity of the raw materials. These catalyst systems are chemically sensitive and may degrade quickly. It has been known for a long time that Cu-oxides display high catalytic activity for oxidation of CO. It was noticed that CuO reduction might be moderated by the presence of Cr ions on the surface. By optimising the Cu content in the catalyst it was found that activity of $CuCr_2O_4$ spinel is comparable to that of Pt and Pd. The traditional preparation of Cu–Cr spinels is rather complicated. Trough SHS CuCr2O4-rich materials were prepared that display better conversion catalytic activity to that displayed by conventional 0.5% Pd/Al_2O_3 systems [34,35].

6. Conclusions

A general description of the SHS process has been made, underling the simplicity of the apparatus for the synthesis, the good quality of the product obtained (due to the high reaction temperature) and the possibility to obtain metastable phases (due to the high reaction rate).

The particle size of the starting powders plays an important role in SHS, it is possible to say that fine particles generally promote the reaction increasing the reaction temperature and the combustion velocity. The starting particle size also influences the grain size of the resulting products.

Density of the compact influences the ignition of the sample. This effect of green density on the ignition and propagation was attributed to the balance between a good particle contact and not too much to lead to excessive heat loss from the reaction zone due to the increased thermal conductivity.

Another aspect is the evolution during reaction of gaseous species, due to the impurity present on the surface of the particle in green compact.

The stoichiometry of the reactants is another important parameter. Generally the deviation from the stoichiometry results in a decrease of the adiabatic

temperature, any excess of either reactants or products will normally decrease the exothermicity of the reaction with consequent reduction of the adiabatic temperature. Addition of a diluent becomes necessary in solid–gas reaction.

The SHS gas–solid reaction can involve different gas for the formation of nitride, hydride and oxide; generally the combustion is promoted when the gas pressure increase. But also in the process where the gas does not participate to the reaction, it influences the combustion.

In some systems there is the inability to establish a self-propagating reaction front due to: (1) low enthalpy reactions, (2) high thermal conductivity of reactants (3) kinetically controlled high enthalpy reactions. So many researchers, in different countries, developed a SHS process coupled with an activation system. In this work three system are considered: (1) Field Activated SHS (FACS) (2) Mechanically Activated SHS (MRS and MASHS) (3) SHS coupled gas-transport. Also in this case the reaction parameters are examined.

The economical and energy saving aspect of the process are reported in final part of the review, with an analysis of environmental impact.

Acknowledgements

The author is grateful to Professor Ignazio Amato (Politecnico of Turin) for his assistance in this work.

References

[1] J.A. Puszynski, Thermochemistry and kinetics, in: A.W. Weimer (Ed.), Carbide, Nitride and Boride Materials Synthesis and Processing, Chapman & Hall, London, 1997, pp. 183–228.
[2] Z.A. Munir, U. Anselmi-Tamburini, Self-propagating exothermic reactions: the synthesis of high-temperature materials by combustion, Materials Science Reports 3 (7) (1989) 277–365.
[3] J.J. Moore, H.J. Feng, Combustion synthesis of advanced materials, Progress in Materials Science 39 (1995) 243–273.
[4] A.G. Merzhanov, History and recent developments in SHS, Ceramics International 21 (1995) 371–379.
[5] C. Bartuli, R.W. Smith, E. Shtessel, SHS powders for thermal spray applications, Ceramics International 23 (1997) 61–68.
[6] M. Mohan Rao, C. Liebenow, M. Jayalakshmi, H. Wulff, U. Guth, F. Scholz, High-temperature combustion synthesis and electrochemical characterization of $LiNiO_2$, $LiCoO_2$ and $LiMn_2O_4$ for lithium-ion secondary batteries, Journal of Solid State Electrochemistry 5 (2001) 348–354.
[7] E.A. Levashov, V.I. Kosayanin, L.M. Krukova, J.J. Moore, D.L. Olson, Structure and properties of Ti–C–B composite thin films produced by sputtering of composite TiC–TiB_2 targets, Surface Coatings Technology 92 (1997) 34–41.
[8] R. Tomasi, Z.A. Munir, Effect of particle size on the reaction wave propagation in the combustion synthesis of Al_2O_3–ZrO_2–Nb composites, Journal of the American Ceramic Society 82 (8) (1999) 1985–1992.
[9] R. Pampuch, Advanced HT ceramic materials via solid combustion, Journal of the European Ceramic Society 19 (1999) 2395–2404.
[10] R. Pampuch, Some fundamental versus practical aspects of self propagating high-temperature synthesis, Solid State Ionics, 101–103 (1997) 899–907.
[11] J.H. Lee, D.H. Seo, W. Won, I.P. Borovinskaya, V.I. Vershinnikov, Combustion characteristics of WO_3/Zn reaction system in SHS process, Journal of Materials Science 36 (2001) 5311–5314.
[12] Y. Li, J. Zhao, J. Han, Self-propagating high temperature synthesis of $Ni_{0.35}Zn_{0.65}Fe_2O_4$ ferrite powders, Materials Research Bulletin 37 (2002) 538–592.
[13] S.D. Dunmead, Processes, in: A.W. Weimer (Ed.), Carbide, Nitride and Boride Materials Synthesis and Processing, Chapman & Hall, London, 1997, pp. 229–272.
[14] I.G. Cano, I.P. Borovinskaya, M.A. Rodriguez, V.V. Grachev, Effect of dilution and porosity on self-propagating high-temperature synthesis of silicon nitride, Journal of the American Ceramic Society 85 (9) (2002) 2209–2211.
[15] S.K. Roy, A. Biswas, Combustion synthesis of TiB and TiB_2 under vacuum, Journal of Materials Science Letters 13 (1994) 371.
[16] S.K. Roy, A. Biswas, S. Banerjee, Self-propagating high-temperature synthesis of titanium borides, Bulletin of Materials Science 16 (5) (1993) 347–356.
[17] D.A. Ponamarev, V.A. Shcherbakov, A.S. Shteinberg, Combustion of thin layers of titanium–boron powder mixture, Doklady Akademii Nauk 340 (5) (1995) 642–645.
[18] M. Eslamloo-Grami, Z.A. Munir, Effect of porosity on the combustion synthesis of titanium nitride, Journal of the American Ceramic Society 73 (5) (1990) 1235–1239.
[19] A.G. Merzhanov, S.Y. Sharivker, Self-propagating high-temperature synthesis of carbides, nitrides and borides, in: Y.G. Gogotsi, R.A. Andrievski (Eds.), Materials Science of Carbides, Nitrides and Borides, Kluwer Academic Publishers, Netherlands, 1999, pp. 205–222.
[20] J.B. Holt, Z.A. Munir, Combustion synthesis of titanium carbide: theory and experiment, Journal of Materials Science 21 (1996) 251–259.
[21] I.G. Cano, S. Pérez Baelo, M.A. Rodriguez, S. de Aza, Self-propagating high temperature-synthesis of Si_3N_4: role of ammonium salt addition, Journal of the European Ceramic Society 21 (2001) 291–295.
[22] A.G. Aleksanyan, S.K. Dolukhanyan, Self-propagating high-temperature synthesis in Y–N–H systems, International Journal of Hydrogen Energy 21 (11-12) (1996) 955–959.
[23] A.G. Aleksanyan, S.K. Dolukhanyan, Combustion of niobium in hydrogen and nitrogen, Synthesis of niobium hydrides and hydridonitrides. International Journal of Hydrogen Energy 26 (2001) 429–433.
[24] L.S. Abovyan, H.H. Nersisyan, S.L. Kharatyan, R. Orrù, R. Saiu, G. Cao, D. Zedda, Synthesis of alumina–silicon carbide composites by chemically activated self-propagating reactions, Ceramics International 27 (2001) 163–169.
[25] Z.A. Munir, Field effects in self-propagating solid-state synthesis reactions, Solid State Ionics 101–103 (1997) 991–1001.
[26] R. Orru, G. Cao, Z.A. Munir, Field-activated combustion synthesis of titanium aluminides, Metallurgical and Materials Transaction A 30A (1999) 1101–1108.
[27] I.J. Shon, D.H. Rho, H.C. Kim, Z.A. Munir, Synthesis of WSi_2–ZrO_2 and WSi_2–Nb composites by field-activated combustion, Journal of Alloy and Compounds 327 (2001) 66–72.
[28] S. Gedevannishvili, Z.A. Munir, The synthesis of TiB_2–$TiAl_3$ composites by field-activated combustion, Materials Science and Engineering A A246 81-85 (1998).
[29] F. Bernard, E. Gaffet, Mechanical alloying in SHS research, International Journal of SHS 10 (2) (2001) 109–132.
[30] T. Kim, M.S. Wooldridge, Catalytically assisted self-propagating high-temperature synthesis of tantalum carbide powders, Journal of the American Ceramic Society 84 (5) (2001) 976–982.

[31] A.G. Merzhanov, Fundamentals, achievements and perspectives for development of solid-flame combustion, Russian Chemical Bulletin 46 (1) (1997) 1–27.
[32] A.G. Merzhanov, Role of ceramics in a self-sustaining environment, Monographs in Materials and Society 4 (1997) 145–161.
[33] G. Cao, R. Orrù, Self-propagating reactions for environmental protection: state of the art and future directions, Chemical Engineering Journal [in press].
[34] G. Xanthopoulou, G. Vekinis, Investigation of catalytic oxidation of carbon monoxide over Cu–Cr-oxide catalyst made by self-propagating high-temperature synthesis, Applied Catalysis B: Environmental 19 (1998) 37–44.
[35] G. Xanthopoulou, G. Vekinis, An overview of some environmental applications of self-propagating high-temperature synthesis, Advances in Environmental Research 5 (2001) 117–128.